

Optimal Temperature Profiles for Nylon 6 Polymerization in Plug-Flow Reactors

A. RAMAGOPAL, ANIL KUMAR, and SANTOSH K. GUPTA, *Department of Chemical Engineering, Indian Institute of Technology, Kanpur, Kanpur-208016, India*

Synopsis

Optimal temperature profiles for nylon 6 polymerization in plug-flow reactors have been obtained under different conditions using a reasonable objective function which gives more flexibility to a designer than those studied earlier. Computations suggest that the temperatures at the feed end of the reactor must be maintained at the highest permissible level (determined by the boiling point of the ϵ -caprolactam) so as to force the degree of polymerization rapidly to the desired value. Thereafter, the temperature should be reduced in order to minimize the undesirable cyclic dimer concentration, and, finally, near the exit of the reactor, the temperature must once again be increased in order to attain higher monomer conversion. The effect of a systematic change of values of the various design variables, one by one, is studied. The profile obtained differs substantially from those obtained by earlier workers because of the differences in the objective function as well as in the kinetic mechanism associated with the formation of the cyclic oligomer. Attempts are also made to obtain a global optimal scheme to produce a polymer of a desired degree of polymerization.

INTRODUCTION

A considerable amount of work has been reported on the simulation of the hydrolytic polymerization of ϵ -caprolactam in various types of reactors.¹⁻¹⁹ This has been reviewed recently.^{1,2} The effects of several operating variables (as, for example, the initial water concentration, temperature, monofunctional acid stabilizers, recycle, backmixing, velocity profile in the reactor, etc.) on the various characteristics of the product stream (like the conversion of the monomer, degree of polymerization \overline{DP} , polydispersity index ρ of the polymer, cyclic oligomer content, etc.) are now well established. In contrast to these simulation studies, little has been reported on the optimization of nylon 6 reactors. Hoftyzer et al.³ were the first to carry out a detailed optimization study of nylon 6 polymerization in plug flow reactors. Using dynamic programming, they computed the optimal temperature and water concentration profiles for producing a polymer of specified \overline{DP} in the shortest reaction time. It was found that the polymerization should be carried out in two stages—the first reactor operating at high temperature and water content and the second one at a low temperature and water content, with an instantaneous removal of water between these stages. For proprietary reasons, however, they presented only qualitative conclusions, which were later shown to be valid by Reimschuessel and Nagasubramanian,⁴ who studied combinations of a two-stage, isothermal, plug-flow reactor system, with water concentration as the main process parameter.

Further studies on the optimization of nylon 6 reactors include those of Naudin ten Cate⁵ and Mochizuki and Ito.⁶ These workers incorporated the formation

of cyclic oligomers in their kinetic scheme and determined optimal temperature profiles required to produce nylon 6 having a fixed value of \overline{DP} , simultaneously minimizing the production of the cyclic compounds⁵ (or attaining a fixed value for it⁶) and maximizing caprolactam conversion. In both of these studies it was found that the temperature of the reactor should first be gradually increased and then gradually lowered. The two optimal temperature profiles obtained by these groups of workers differed markedly due to the objective functions being different as well as the reaction mechanism for the formation of cyclic oligomers being different. Once again, only qualitative results were presented for proprietary reasons. Also, the kinetics of the cyclic oligomer formation step used by these workers was not entirely appropriate.

In all the four optimization studies discussed above, the objective function was chosen so as to obtain a polymer having fixed values of \overline{DP} and cyclic oligomer content, and the final conversions were usually chosen very close to equilibrium values. These studies are, therefore, of immense importance to a nylon 6 plant which is in operation, where an engineer may wish to change the grade of the polymer produced at times. An engineer designing a new nylon 6 plant, on the other hand, has much more flexibility in choosing the design and control variables,² and the objective functions that he may wish to optimize may be very different from the ones studied till now. In this study, one such objective function is being considered which is of more relevance in the *design* of a new plant than in the optimal *operation* of established plants. It may be added that a considerable amount of work has been reported and compiled^{20,21} in the literature on the optimization of nonpolymeric reactors, in which a whole array of objective functions and their effects on the control variable profiles have been studied. Indeed, Hicks et al.²² have studied the optimization of general ARB-type condensation polymerizations using some of these objective functions while Kumar et al.²³ have optimized the first stage of PET reactors using similar functions.

In recent years, considerable progress has been made in the modeling and simulation of nylon 6 reactors,^{7-17,24} and the rate and equilibrium constants for the various reactions in the kinetic scheme (and, in particular, cyclic oligomer formation) have been determined with precision.^{7,8} This major new development, coupled with the sensitivity of the optimal temperature profile to the objective function and the kinetic scheme, establishes the need for detailed and systematic studies on the optimization of nylon 6 reactors using various types of objective functions and constraints. In this paper, we have proposed one such objective function which is more flexible than those used earlier and so is of relevance at the design stage, and have obtained optimal temperature profiles.

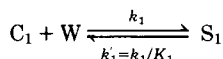
FORMULATION

The kinetic scheme used in this work is given in Table I along with the relevant rate and equilibrium constants.⁷⁻¹¹ This scheme represents the more recent and precise information on nylon 6 polymerization that is available in the literature. In addition to the three major reactions, ring-opening, polycondensation, and polyaddition, it also incorporates reaction with monofunctional acid stabilizers and also two reactions of the cyclic dimer. Reactions with higher cyclic

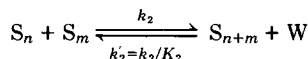
oligomers are not incorporated in this scheme since equally precise experimental information is not available on these, but this does not represent any serious problem since it is well established^{7-11,18,19} that the cyclic dimer constitutes the

TABLE I
Kinetic Scheme and Data⁷⁻¹¹ for Nylon 6 Polymerization^a

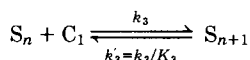
1. Ring opening



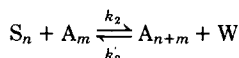
2. Polycondensation



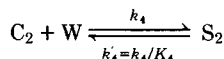
3. Polyaddition



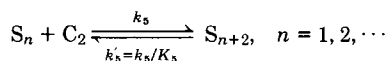
4. Reaction with monofunctional acid



5. Ring opening of cyclic dimer



6. Polyaddition of cyclic dimer



Rate and Equilibrium Constants

$$k_i = A_i^0 \exp(-E_i^0/RT) + A_i^f \exp(-E_i^f/RT) \sum_{n=1}^{\infty} ([A_n] + [S_n])$$

$$\equiv k_i^0 + k_i^f \sum_{n=1}^{\infty} ([S_n] + [A_n])$$

$$K_i = \exp[(\Delta S_i - \Delta H_i/T)/R], \quad i = 1, 2, \dots, 5$$

<i>i</i>	A_i^0 (kg/mol · h)	E_i^0 (cal/mol)	A_i^f (kg ² /mol ² · h)	E_i^f (cal/mol)	ΔH_i (cal/mol)	ΔS_i (eu)
1	5.9874×10^5	1.9880×10^4	4.3075×10^7	1.8806×10^4	1.9180×10^3	-7.8846×10^0
2	1.8942×10^{10}	2.3271×10^4	1.2114×10^{10}	2.0670×10^4	-5.9458×10^3	9.4374×10^{-1}
3	2.8558×10^9	2.2845×10^4	1.6377×10^{10}	2.0107×10^4	-4.0438×10^3	-6.9457×10^0
4	8.5778×10^{11}	4.2000×10^4	2.3307×10^{12}	3.7400×10^4	-9.6000×10^3	-1.4520×10^1
5	2.5701×10^8	2.1300×10^4	3.0110×10^9	2.0400×10^4	-3.1691×10^3	5.8265×10^{-1}

^a C₁: ε-caprolactam; C₂: $\text{H}-\text{N}(\text{CH}_2)_5-\text{C}(\text{O})\text{N}(\text{CH}_2)_5-\text{C}(\text{O})\text{H}$; W: water; S_{*n*}: $\text{H}-\text{N}(\text{CH}_2)_5-\text{C}(\text{O})\text{N}(\text{CH}_2)_5-\text{C}(\text{O})\text{N}(\text{CH}_2)_5-\text{C}(\text{O})\text{N}(\text{CH}_2)_5-\text{C}(\text{O})\text{N}(\text{CH}_2)_5-\text{C}(\text{O})\text{H}$; A_{*n*}: $\text{X}-\text{C}(\text{O})\text{N}(\text{CH}_2)_5-\text{C}(\text{O})\text{H}$, X unreactive group; T = temperature; R = gas constant.

major share of the cyclic compounds in the reaction mass. The corresponding mass balance equations are given in Table II. These represent the equations for the state variables x_1, x_2, \dots, x_{10} defined in Table II. The balance equations require approximations to "close" the hierarchy of equations and the closure

TABLE II
Mass Balance Equations (State Variable Equations)^{a,b}

$$\begin{aligned} \dot{x}_1 &\equiv \frac{d[C_1]}{dt} = -k_1[C_1][W] + k'_1[S_1] - k_3[C_1]\mu_0 + k'_3(\mu_0 - [S_1]) \\ \dot{x}_2 &\equiv \frac{d[S_1]}{dt} = k_1[C_1][W] - k'_1[S_1] - 2k_2[S_1]\mu_0 + 2k'_2[W](\mu_0 - [S_1]) \\ &\quad - k_3[S_1][C_1] + k'_3[S_2] - k_2\mu'_0[S_1] + k'_2[W](\mu'_0 - [A_1]) \\ &\quad - k_5[S_1][C_2] + k'_5[S_3] \\ \dot{x}_3 &\equiv \frac{d\mu_0}{dt} = k_1[C_1][W] - k'_1[S_1] - k_2\mu_0^2 + k'_2[W](\mu_1 - \mu_0) \\ &\quad - k_2\mu_0\mu'_0 + k'_2[W](\mu'_1 - \mu'_0) + k_4[W][C_2] - k'_4[S_2] \\ \dot{x}_4 &\equiv \frac{d\mu_1}{dt} = k_1[C_1][W] - k'_1[S_1] + k_3[C_1]\mu_0 - k'_3(\mu_0 - [S_1]) \\ &\quad - k_2\mu'_0\mu_1 - \frac{1}{2}k'_2[W](\mu'_1 - \mu'_0) + 2k_5[C_2]\mu_0 \\ &\quad - 2k'_5(\mu_0 - [S_1] - [S_2]) + 2k_4[W][C_2] - 2k'_4[S_2] \\ \dot{x}_5 &\equiv \frac{d\mu_2}{dt} = k_1[C_1][W] - k'_1[S_1] + 2k_2\mu_1^2 + \frac{1}{3}k'_2[W](\mu_1 - \mu_3) \\ &\quad + k_3[C_1](\mu_0 + 2\mu_1) + k'_3(\mu_0 - 2\mu_1 + [S_1]) \\ &\quad - k_2\mu_2\mu'_0 + \frac{1}{6}k'_2[W](2\mu'_3 - 3\mu'_2 + \mu'_1) \\ &\quad + 4k_5[C_2](\mu_1 + \mu_0) + 4k'_5(\mu_0 - \mu_1 + [S_2]) + 4k_4[W][C_2] - 4k'_4[S_2] \\ \dot{x}_6 &\equiv \frac{d[C_2]}{dt} = -k_4[C_2][W] + k'_4[S_2] - k_5[C_2]\mu_0 + k'_5(\mu_0 - [S_1] - [S_2]) \\ \dot{x}_7 &\equiv \frac{d[W]}{dt} = -k_1[C_1][W] + k'_1[S_1] + k_2(\mu_0)^2 - k'_2[W](\mu_1 - \mu_0) \\ &\quad + k_2\mu_0\mu'_0 - k'_2[W](\mu'_1 - \mu'_0) - k_4[C_2][W] + k'_4[S_2] \\ \dot{x}_8 &\equiv \frac{d\mu'_1}{dt} = k_2\mu_1\mu'_0 - \frac{1}{2}k'_2[W](\mu'_2 - \mu'_1) \\ \dot{x}_9 &\equiv \frac{d\mu'_2}{dt} = k_2(2\mu_1\mu'_1 + \mu_2\mu'_0) - \frac{1}{6}k'_2[W](4\mu'_3 - 3\mu'_2 - \mu'_1) \\ \dot{x}_{10} &\equiv \frac{d[A_1]}{dt} = -k_2[A_1]\mu_0 + k'_2[W](\mu'_0 - [A_1]) \end{aligned}$$

^a Closure conditions¹⁰: $[S_2] = [S_3] = [S_1]$;

$$\mu_3 = \mu_2(2\mu_2\mu_0 - \mu_1^2)/\mu_1\mu_0, \quad \mu'_3 = \mu'_2(2\mu'_2\mu'_0 - \mu_1'^2)/\mu_1\mu'_0$$

^b $\mu_k \equiv \sum_{n=1}^{\infty} n^k [S_n]$, $\mu'_k \equiv \sum_{n=1}^{\infty} n^k [A_n]$, $k = 0, 1, 2, 3$

$$\frac{d\mu'_0}{dt} = 0 \quad \text{or} \quad \mu'_0 = \text{const} (= \text{inlet value})$$

conditions used by Tai et al.¹⁰ are also included in this table. These closure equations have been demonstrated to be extremely successful in predicting the moments for both batch (or plug-flow) reactors¹⁵ as well as continuous-flow stirred-tank reactors¹⁶ and give results which match with those obtained from a detailed integration of mass balance equations of the individual species.^{13,14}

The objective function $I\{T(t)\}$ selected in this work is

$$\text{minimize } I\{T(t)\} = \alpha_3[C_1(t_f)] + \int_0^{t_f} \left\{ \frac{\alpha_2}{\overline{DP}_d^2} \left(\frac{\mu_1 + \mu_1'}{\mu_0 + \mu_0'} - \overline{DP}_d \right)^2 + \alpha_1[C_2]^2 \right\} dt \quad (1)$$

where $T(t)$ is the temperature profile (temperature as a function of residence time in a plug-flow reactor or temperature as a function of time in a batch reactor) to be determined optimally so that I is minimized, t_f is the total residence or reaction time, \overline{DP}_d is the desired value of the degree of polymerization of the polymer to be manufactured, and α_1 , α_2 , and α_3 are weighting factors representing the relative importance of cyclic dimer, unconverted caprolactam, and \overline{DP} of the product in the objective function. The above objective function tends to bring the product \overline{DP} as close to the desired value \overline{DP}_d in as short a reaction time as possible while simultaneously minimizing the unconverted caprolactam and the cyclic dimer concentration in the product. The objective function chosen is thus similar, but not identical to those used by Naudin ten Cate⁵ and Mochizuki and Ito⁶ (who constrained the final \overline{DP} to a *fixed* value). The function chosen in eq. (1) allows more flexibility in the optimal design of nylon 6 reactors while simultaneously causing the product degree of polymerization to lie *close to* (but not necessarily equal to) a desired value. This is because an engineer can usually tolerate a few percent deviation in the value of \overline{DP} without jeopardizing the product physical properties appreciably.

In order to determine the optimal temperature profile, we define Hamiltonian H , which, for the present system, becomes

$$H = \alpha_1[C_2]^2 + \frac{\alpha_2}{\overline{DP}_d^2} \left(\frac{\mu_1 + \mu_1'}{\mu_0 + \mu_0'} - \overline{DP}_d \right)^2 + \sum_{i=1}^{10} \lambda_i \dot{x}_i(x_1, x_2, \dots, x_{10}, T) \quad (2)$$

where λ_i are the adjoint functions given by

$$-\frac{d\lambda_i}{dt} = \frac{\partial H}{\partial x_i}, \quad i = 1, 2, \dots, 10 \quad (3)$$

with the "final" conditions as

$$\lambda_i(t_f) = \frac{\partial}{\partial x_i} \{ \alpha_3[C_1] \}_{t=t_f} \quad (4)$$

The detailed equations for the λ 's are given in Table III.

The optimal temperature profile is obtained under the following necessary conditions:

$$\frac{\partial H}{\partial T} = 0 = \sum_{i=1}^{10} \lambda_i \frac{\partial \dot{x}_i(x_1, x_2, \dots, x_{10}, T)}{\partial T} \quad (5)$$

The detailed equations for $\partial \dot{x}_i / \partial T$ are given in Table IV.

TABLE III
Equations for the Adjoint Functions^a

$$\begin{aligned}
 -\frac{d\lambda_1}{dt} &= (k_1[W] + k_3\mu_0)(-\lambda_1 + \lambda_4 + \lambda_5) + k_1[W](\lambda_2 + \lambda_3 - \lambda_7) \\
 &\quad - k_3[S_1]\lambda_2 + 2k_3\mu_1\lambda_5 \\
 -\frac{d\lambda_2}{dt} &= \frac{k_1}{K_1}(\lambda_1 - \lambda_2 - \lambda_3 - \lambda_4 - \lambda_5 + \lambda_7) + \frac{k_3}{K_3}(-\lambda_1 + \lambda_4 + \lambda_5) \\
 &\quad + \frac{k_5}{K_5}(2\lambda_4 - \lambda_6) + \lambda_2(-2k_2\mu_0 - 2\frac{k_2}{K_2}[W] - k_2\mu'_0 - k_3[C_1] - k_5[C_2]) \\
 -\frac{d\lambda_3}{dt} &= \left(k_3[C_1] - \frac{k_3}{K_3}\right)(-\lambda_1 + \lambda_4) + \left(k_3[C_1] + \frac{k_3}{K_3}\right)(\lambda_5) \\
 &\quad + \left(k_2[S_1] - \frac{k_2}{K_2}[W]\right)(-2\lambda_2) + \left(2k_2\mu_0 + \frac{k_2}{K_2}[W] + k_2\mu'_0\right)(-\lambda_3 + \lambda_7) \\
 &\quad + \left(k_5[C_2] - \frac{k_5}{K_5}\right)(2\lambda_4 - \lambda_6) + \left(k_5[C_2] + \frac{k_5}{K_5}\right)(4\lambda_5) - k_2[A_1]\lambda_{10} \\
 &\quad + k_1\left([C_1][W] - \frac{[S_1]}{K_1}\right)(-\lambda_1 + \lambda_2 + \lambda_3 + \lambda_4 + \lambda_5 - \lambda_7) \\
 &\quad + k_2\left(\mu_0^2 + \mu_0\mu'_0 - \frac{[W](\mu_1 - \mu_0)}{K_2} - \frac{[W](\mu'_1 - \mu'_0)}{K_2}\right)(-\lambda_3 + \lambda_7) \\
 &\quad + k_3\left(\mu_0[C_1] - \frac{\mu_0 - [S_1]}{K_3}\right)(-\lambda_1 + \lambda_4) \\
 &\quad + k_4\left([W][C_2] - \frac{[S_2]}{K_4}\right)(\lambda_3 + 2\lambda_4 + 4\lambda_5 - \lambda_6 - \lambda_7) \\
 &\quad - 2k_5\lambda_2\left(\mu_0[S_1] - \frac{[W](\mu_0 - [S_1])}{K_2} + \frac{\mu'_0[S_1]}{2} - [W]\frac{\mu'_0 - [A_1]}{2K_2}\right) \\
 &\quad - k_5\lambda_4\left(\mu_1\mu'_0 + \frac{[W](\mu'_1 - \mu'_2)}{2K_2}\right) + 2k_5\lambda_5\left(\mu_1^2 + [W]\frac{\mu_1 - \mu_3}{6K_2}\right) \\
 &\quad - k_5\lambda_5\left(\mu_2\mu'_0 - \frac{[W](2\mu'_3 - 3\mu'_2 + \mu'_1)}{6K_2}\right) + k_5\lambda_8\left(\mu_1\mu'_0 - \frac{[W](\mu'_2 - \mu'_1)}{2K_2}\right) \\
 &\quad + k_5\lambda_9\left(2\mu_1\mu'_1 + \mu_2\mu'_0 - \frac{[W](4\mu'_3 - 3\mu'_2 - \mu'_1)}{6K_2}\right) \\
 &\quad - k_5\lambda_{10}\left(\mu_0[A_1] - [W]\frac{\mu'_0 - [A_1]}{K_2}\right) - k_5\lambda_2\left([C_1][S_1] - \frac{[S_2]}{K_3}\right) \\
 &\quad + k_5\lambda_5\left(\mu_0 + 2\mu_1\right)[C_1] + \frac{\mu_0 - 2\mu_1 + [S_1]}{K_3} \\
 &\quad - k_5\lambda_2\left([S_1][C_2] - \frac{[S_3]}{K_5}\right) + k_5\left([C_2]\mu_0 - \frac{\mu_0 - [S_1] - [S_2]}{K_5}\right)(2\lambda_4 - \lambda_6) \\
 &\quad + 4k_5\lambda_5\left([C_2](\mu_1 + \mu_0) + \frac{\mu_0 - \mu_1 + [S_2]}{K_5}\right) \\
 &\quad - \frac{2\alpha_2}{\overline{DP}_d^2}\left(\frac{\mu_1 + \mu'_1}{\mu_0 + \mu'_0} - \overline{DP}_d\right)\frac{\mu_1 + \mu'_1}{(\mu_0 + \mu'_0)^2} \\
 -\frac{d\lambda_4}{dt} &= \frac{k_2[W]}{K_2}\left(\lambda_3 + \frac{\lambda_5}{3} - \lambda_7\right) + k_2\mu'_0(-\lambda_4 + \lambda_8) \\
 &\quad + \left(2k_3[C_1] - 2\frac{k_3}{K_3} + 4k_5[C_2] - \frac{4k_5}{K_5} + 4k_2\mu_1\right)\lambda_5
 \end{aligned}$$

TABLE III. (Continued from the previous page.)

$$\begin{aligned}
 & + 2k_2\mu'_1\lambda_9 + \frac{2\alpha_2}{\overline{DP}_d^2} \left(\frac{\mu_1 + \mu'_1}{\mu_0 + \mu'_0} - \overline{DP}_d \right) \frac{1}{\mu_0 + \mu'_0} \\
 - \frac{d\lambda_5}{dt} & = k_2\mu'_0(\lambda_9 - \lambda_5) \\
 - \frac{d\lambda_6}{dt} & = k_4[W](\lambda_3 + 2\lambda_4 + 4\lambda_5 - \lambda_6 - \lambda_7) + k_5\mu_0(2\lambda_4 + 4\lambda_5 - \lambda_6) \\
 & \quad - k_5[S_1]\lambda_2 + 4k_5\mu_1\lambda_5 + 2\alpha_1[C_2] \\
 - \frac{d\lambda_7}{dt} & = k_1[C_1](-\lambda_1 + \lambda_2 + \lambda_3 + \lambda_4 + \lambda_5 - \lambda_7) + k_4[C_2](\lambda_3 + 2\lambda_4 + 4\lambda_5 - \lambda_6 - \lambda_7) \\
 & \quad + \frac{k_2}{K_2}(\mu_1 - \mu_0)(\lambda_3 - \lambda_7) + \frac{k_2}{K_2}(\mu'_1 - \mu'_0)(\lambda_3 - \lambda_7) \\
 & \quad + \frac{k_2}{K_2} \left(2(\mu_0 - [S_1])\lambda_2 + (\mu'_0 - [A_1])(\lambda_2 + \lambda_{10}) - \frac{\mu'_1 - \mu'_2}{2}(\lambda_4 - \lambda_8) \right. \\
 & \quad \left. + \frac{\mu_1 - \mu_3}{3}\lambda_5 + \frac{2\mu'_3 - 3\mu'_2 + \mu'_1}{6}\lambda_5 - \frac{4\mu'_3 - 3\mu'_2 - \mu'_1}{6}\lambda_9 \right) \\
 - \frac{d\lambda_8}{dt} & = \frac{k_2}{K_2} [W] \left(\lambda_3 - \frac{\lambda_4}{2} + \frac{\lambda_5}{6} - \lambda_7 + \frac{\lambda_8}{2} + \frac{\lambda_9}{6} \right) + 2k_2\mu_1\lambda_9 \\
 & \quad + \frac{2\alpha_2}{\overline{DP}_d^2} \left(\frac{\mu_1 + \mu'_1}{\mu_0 + \mu'_0} - \overline{DP}_d \right) \frac{1}{\mu_0 + \mu'_0} \\
 - \frac{d\lambda_9}{dt} & = \frac{k_2[W]}{2K_2} (\lambda_4 - \lambda_5 - \lambda_8 + \lambda_9) \\
 - \frac{d\lambda_{10}}{dt} & = \frac{k_2[W]}{K_2} (-\lambda_2 - \lambda_{10}) - k_2\mu_0\lambda_{10}
 \end{aligned}$$

^a Boundary conditions:

$$\begin{aligned}
 \lambda_1(t_f) & = \alpha_3, \quad \lambda_2(t_f) = 0, \quad \lambda_3(t_f) = 0, \quad \lambda_4(t_f) = 0 \\
 \lambda_5(t_f) & = 0, \quad \lambda_6(t_f) = 0, \quad \lambda_7(t_f) = 0, \quad \lambda_8(t_f) = 0 \\
 \lambda_9(t_f) & = 0, \quad \lambda_{10}(t_f) = 0
 \end{aligned}$$

In obtaining the various equations in Tables III and IV, the closure equations of Table II have *not* been substituted in the equations for \dot{x}_i while differentiating them with respect to x_j (to obtain $d\lambda_i/dt$). Thus, in computing dx_5/dx_2 , for example, $\partial[S_2]/\partial[S_1]$ has been taken as zero instead of unity. It is expected that differentiation after substitution of the closure equations will not give substantially different results.

In obtaining the optimal temperature profiles, the control variable (temperature) is constrained to lie between two limiting values³

$$220^\circ\text{C} \leq T \leq 270^\circ\text{C} \tag{6}$$

The lower of these values represents the melting point of the polymer, and the upper limit represents the approximate boiling point of (pure) caprolactam at atmospheric conditions.

In order to obtain the optimal temperature profile, the control vector iteration procedure suggested by Ray and Szekely²⁰ has been used. In this technique, one assumes a temperature profile $T_0(t)$, integrates the state variable equations

TABLE IV
 Terms $\partial \dot{x}_i / \partial T$ Required in Eq. (5)

$$\begin{aligned} \frac{\partial \dot{x}_1}{\partial T} &= -k_1^* \left([W][C_1] - \frac{[S_1]}{K_1} \right) - \frac{k_1 K_1^*}{K_1^2} [S_1] - k_3^* \left(\mu_0 [C_1] - \frac{\mu_0 - [S_1]}{K_3} \right) \\ &\quad - \frac{k_3 K_3^*}{K_3^2} (\mu_0 - [S_1]) \\ \frac{\partial \dot{x}_2}{\partial T} &= k_1^* \left([W][C_1] - \frac{[S_1]}{K_1} \right) + \frac{k_1 K_1^*}{K_1^2} [S_1] - 2k_2^* \left(\mu_0 [S_1] - \frac{[W](\mu_0 - [S_1])}{K_2} \right) \\ &\quad + \frac{\mu_0' [S_1]}{2} - \frac{[W](\mu_0' - [A_1])}{2K_2} - \frac{2k_2 K_2^* [W]}{K_2^2} \left(\mu_0 - [S_1] + \frac{\mu_0' - [A_1]}{2} \right) \\ &\quad - k_3^* \left([C_1][S_1] - \frac{[S_2]}{K_3} \right) - \frac{k_3 K_3^*}{K_3^2} [S_2] - k_5^* \left([C_2][S_1] - \frac{[S_3]}{K_5} \right) \\ &\quad - \frac{k_5 K_5^*}{K_5^2} [S_3] \\ \frac{\partial \dot{x}_3}{\partial T} &= k_1^* \left([W][C_1] - \frac{[S_1]}{K_1} \right) + \frac{k_1 K_1^*}{K_1^2} [S_1] - k_2^* \left(\mu_0^2 - \frac{[W](\mu_1 - \mu_0)}{K_2} \right) \\ &\quad + \mu_0 \mu_0' - \frac{[W](\mu_1' - \mu_0')}{K_2} - \frac{k_2 K_2^*}{K_2^2} [W](\mu_1 + \mu_1' - \mu_0 - \mu_0') \\ &\quad + k_4^* \left([W][C_2] - \frac{[S_2]}{K_4} \right) + \frac{k_4 K_4^*}{K_4^2} [S_2] \\ \frac{\partial \dot{x}_4}{\partial T} &= k_1^* \left([W][C_1] - \frac{[S_1]}{K_1} \right) + \frac{k_1 K_1^*}{K_1^2} [S_1] + k_3^* \left(\mu_0 [C_1] - \frac{\mu_0 - [S_1]}{K_3} \right) \\ &\quad + \frac{k_3 K_3^*}{K_3^2} (\mu_0 - [S_1]) + 2k_4^* \left([W][C_2] - \frac{[S_2]}{K_4} \right) + \frac{2k_4 K_4^*}{K_4^2} [S_2] \\ &\quad + 2k_5^* \left(\mu_0 [C_2] - \frac{\mu_0 - [S_1] - [S_2]}{K_5} \right) + \frac{2k_5 K_5^*}{K_5^2} (\mu_0 - [S_1] - [S_2]) \\ &\quad - k_2^* \left(\mu_0 \mu_1 + \frac{[W](\mu_1' - \mu_2')}{2K_2} \right) + \frac{k_2 K_2^*}{2K_2^2} [W](\mu_1' - \mu_2') \\ \frac{\partial \dot{x}_5}{\partial T} &= k_1^* \left([W][C_1] - \frac{[S_1]}{K_1} \right) + \frac{k_1 K_1^*}{K_1^2} [S_1] + \frac{k_2^* [W](\mu_1 - \mu_3)}{3K_2} - \frac{k_2 K_2^*}{3K_2^2} (\mu_1 - \mu_3) \\ &\quad + k_3^* \left([C_1](2\mu_1 + \mu_0) + \frac{\mu_0 - 2\mu_1 + [S_1]}{K_3} \right) - \frac{k_3 K_3^*}{K_3^2} (\mu_0 - 2\mu_1 + [S_1]) \\ &\quad + 4k_5^* \left([C_2](\mu_0 + \mu_1) + \frac{\mu_0 - \mu_1 + [S_2]}{K_5} \right) - \frac{4k_5 K_5^*}{K_5^2} (\mu_0 - \mu_1 + [S_2]) \\ &\quad + 4k_4^* \left([W][C_2] - \frac{[S_2]}{K_4} \right) + \frac{4k_4 K_4^*}{K_4^2} [S_2] \\ &\quad + k_2^* \left(2\mu_1^2 - \mu_2 \mu_0 + \frac{[W](2\mu_3 - 3\mu_2 + \mu_1)}{6K_2} \right) - \frac{k_2 K_2^*}{6K_2^2} [W](2\mu_3 - 3\mu_2 + \mu_1) \\ \frac{\partial \dot{x}_6}{\partial T} &= -k_4^* \left([W][C_2] - \frac{[S_2]}{K_4} \right) - \frac{k_4 K_4^*}{K_4^2} [S_2] - k_5^* \left(\mu_0 [C_2] - \frac{\mu_0 - [S_1] - [S_2]}{K_5} \right) \\ &\quad - \frac{k_5 K_5^*}{K_5^2} (\mu_0 - [S_1] - [S_2]) \\ \frac{\partial \dot{x}_7}{\partial T} &= -k_1^* \left([W][C_1] - \frac{[S_1]}{K_1} \right) - \frac{k_1 K_1^*}{K_1^2} [S_1] + k_2^* \left(\mu_0^2 - \frac{[W](\mu_1 - \mu_0)}{K_2} \right) + \mu_0 \mu_0' \\ &\quad - \frac{[W](\mu_1' - \mu_0')}{K_2} + \frac{k_2 K_2^*}{K_2^2} [W](\mu_1 - \mu_0 + \mu_1' - \mu_0') \end{aligned}$$

TABLE IV. (Continued from the previous page.)

$$\begin{aligned}
 & -k_4^* \left([W][C_2] - \frac{[S_2]}{K_4} \right) - \frac{k_4 K_4^*}{K_4^2} [S_2] \\
 \frac{\partial \dot{x}_8}{\partial T} &= k_2^* \left(\mu_1 \mu'_0 - \frac{[W](\mu'_2 - \mu'_1)}{2K_2} \right) + \frac{k_2 K_2^*}{2K_2^2} [W](\mu'_2 - \mu'_1) \\
 \frac{\partial \dot{x}_9}{\partial T} &= k_2^* \left(2\mu_1 \mu'_1 + \mu_2 \mu'_0 - \frac{[W](4\mu'_3 - 3\mu'_2 - \mu'_1)}{6K_2} \right) \\
 & \quad + \frac{k_2 K_2^*}{6K_2^2} [W](4\mu'_3 - 3\mu'_2 - \mu'_1) \\
 \frac{\partial \dot{x}_{10}}{\partial T} &= k_2^* \left(-\mu_0 [A_1] + \frac{[W](\mu'_0 - [A_1])}{K_2} \right) - \frac{k_2 K_2^*}{K_2^2} [W](\mu'_0 - [A_1])
 \end{aligned}$$

where

$$k_i^* \equiv \frac{\partial k_i}{\partial T} = \{E_i^0 k_i^0 + E_i^* k_i^*(\mu_0 + \mu'_0)\} / RT^2, \quad i = 1, 2, \dots, 5$$

and

$$K_i^* \equiv \frac{\partial K_i}{\partial T} = K_i(\Delta H_i) / RT^2, \quad i = 1, 2, \dots, 5$$

(Table II) in the forward direction (from $t = 0$ to t_f , storing the values of $x_1, x_2, \dots, x_{10}, \partial \dot{x}_1 / \partial T, \dots, \partial \dot{x}_{10} / \partial T$), computes the objective function and the values of the adjoint functions λ_i at $t = t_f$, integrates the adjoint function equations (Table III) in the reverse direction (from t_f to 0), and finally corrects the temperature profile using

$$\begin{aligned}
 T^{(\text{new})}(t) &= T^{(\text{old})}(t) - \epsilon \left(\frac{\partial H}{\partial T} \right) \\
 &= T^{(\text{old})}(t) - \epsilon \sum_{i=1}^{10} \lambda_i \frac{\partial \dot{x}_i}{\partial T} \tag{7}
 \end{aligned}$$

where ϵ is assumed to be independent of time t . This completes one iteration of computation. It may be mentioned that $\partial H / \partial T$ in eq. (7) will not necessarily be zero since the assumed temperature profile is not optimal. The fourth-order Runge-Kutta method was used for integration.

Several methods of choosing ϵ have been suggested in the literature.^{20,21} What we have attempted is a slight modification of the method suggested by Ray and Szekely.²⁰ Several values of ϵ are selected, thus generating different temperature profiles, and, after an iteration, the state variable equations are integrated in the forward direction to obtain the corresponding values of the objective functions. The (approximate) value of ϵ which gives the lowest value of the objective function is selected, and the next iteration is carried out using the corresponding temperature profile. Thus, our procedure requires an interactive computer terminal so as to feed in values of ϵ at each iteration. This procedure had to be adopted since the method of fitting a quadratic function to the objective function²⁰ led to severe numerical instabilities. Also, our technique was considerably more rapid than that suggested by Denn,²¹ which does not require an interactive computer terminal. This above procedure is repeated till the value of the ob-

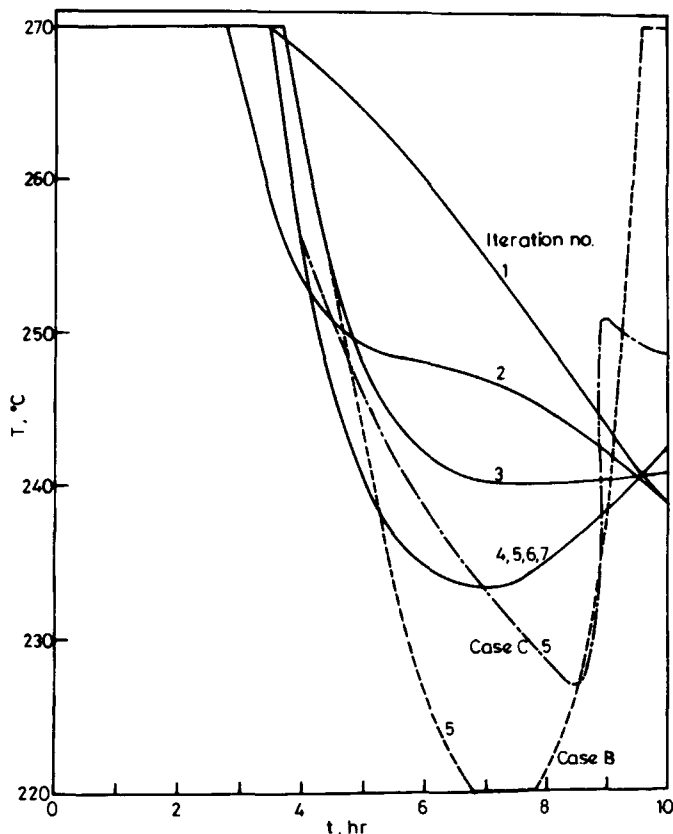


Fig. 1. Variation of temperature profile with iteration: (—, case A) initial guess isothermal at 237°C ($I = 2995$); (---, case B) fifth iteration with initial guess isothermal at 270°C ($I = 2989$); (-·-·, case C) fifth iteration with nonisothermal initial temperature profile ($T = 270^\circ\text{C}$, $0 \leq t \leq 3.5$ h; $T = 223^\circ\text{C}$, $3.5 \leq t \leq 9$; $T = 244^\circ\text{C}$, $9 \leq t \leq 10$; $I = 2999$).

jective function does not change significantly (at this point, $\partial H/\partial T$ should rigorously be zero).

The value of Δt used for integration is chosen such that there are 1000 intervals between $0 \leq t \leq t_f$. In order to reduce memory storage requirements, the values of T , λ 's, and $\partial H/\partial T$ are stored at only 100 equally spaced points between $0 \leq t \leq t_f$, and linear interpolation is used.²⁰ Several checks were used to ensure that the results are free of errors. The computer program gave results which matched those obtained earlier¹⁵ under isothermal conditions. Also, independent checks on the stoichiometric balances¹⁵ on $(-\text{CH}_2)_5-$ units and water were made at every stage and these were found to lie within about 10⁻⁵% of the theoretical values. In addition, our computer program gave results identical to those obtained by Ray and Szekely²⁰ (Example 6.5.2) when the corresponding equations were used. All these checks gave confidence regarding the correctness of the computer program.

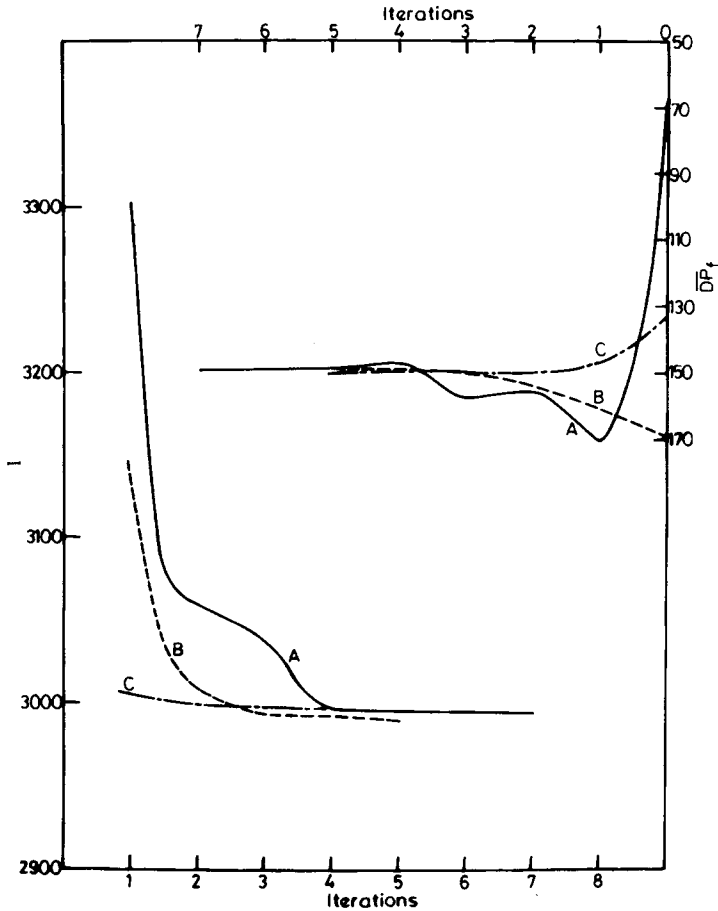


Fig. 2. Variation of I and \overline{DP}_f with iteration for cases A, B, and C (as in Fig. 1).

RESULTS AND DISCUSSION

A very systematic parametric study was made to obtain the effect of each of the parameters on the optimal temperature profile. The following conditions were used for the "reference" run:

$$[C_1]_0 = 8.8 \text{ mol/kg mixture}$$

$$[W]_0 = 0.16 \text{ mol/kg}, \quad [A_1]_0 = 0 \text{ (feed of pure caprolactam and water)}$$

$$\alpha_1 = 10^6, \quad \alpha_2 = 10^3, \quad \alpha_3 = 50, \quad \overline{DP}_d = 140, \quad t_f = 10 \text{ h} \quad (8)$$

where the subscript 0 indicates feed conditions. Figure 1 shows how the temperature profile changes from iteration to iteration when the starting (assumed) profile is isothermal at 237°C . It is observed that the profile is essentially unchanged after the fourth iteration. The effect of the initial guess is also shown in this figure. It is found that the converged results are slightly sensitive to the initial guess, even though the numerical value of the objective function differs

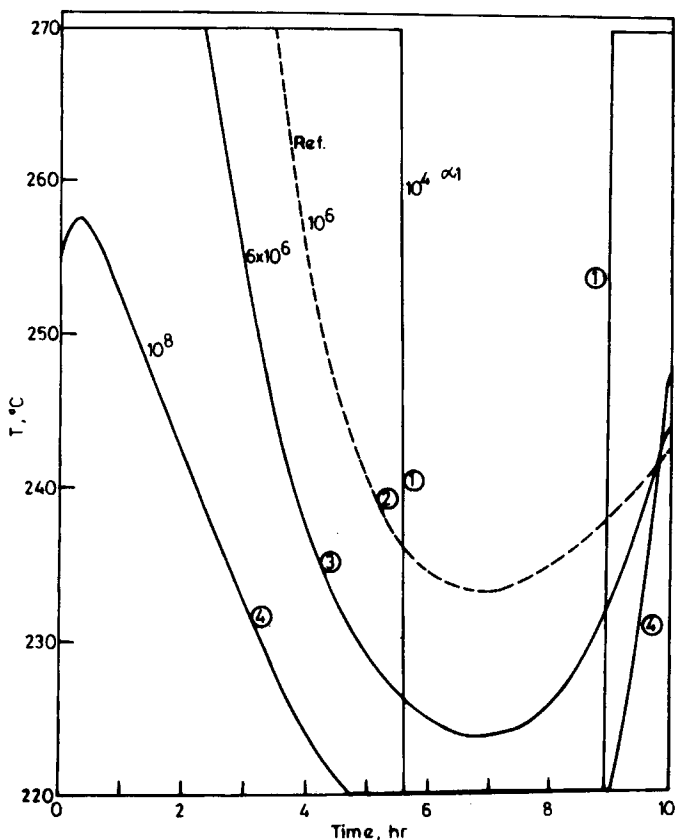


Fig. 3. Effect of α_1 on the optimal temperature profiles. Other parameters are the same as in eq. (8). Values of final conversion (%), \overline{DP}_f , and $[C_2(t_f)]$ are: (1) 82.7, 152.5, 0.0135; (2) 76.7, 144.6, 0.0101; (3) 67, 117, 0.00725; (4) 29.3, 50.6, 0.00213. Curve 2 represents reference conditions.

by less than a $\frac{1}{3}\%$, as illustrated in Figure 2, where it is also shown that the final value \overline{DP}_f of the degree of polymerization is relatively insensitive to the optimal temperature profile. Such a behavior is characteristic of this optimization algorithm,²⁰ and Denn²¹ states that this insensitivity of the objective function to the final temperature profile is indeed a blessing in disguise for an engineer. In this paper, an isothermal initial profile with $T = 237^\circ\text{C}$ is used for all runs hereafter. It may be added that second-order techniques, which are computationally and conceptually more difficult as well as sensitive to convergence problems, can, at times, give better results. Figure 1 clearly establishes that the optimal temperature profile has an initial region at the highest permissible temperature; then the temperature drops, the slope and the magnitude depending upon the values of the various parameters, and, finally, the temperature again increases. This behavior is in contrast to that observed by Naudin ten Cate⁵ and Mochizuki and Ito,⁶ whose optimal temperature profiles increase from the lowest value and then drop back. Our objective function differs significantly from those of earlier studies in which the caprolactam conversion was minimized

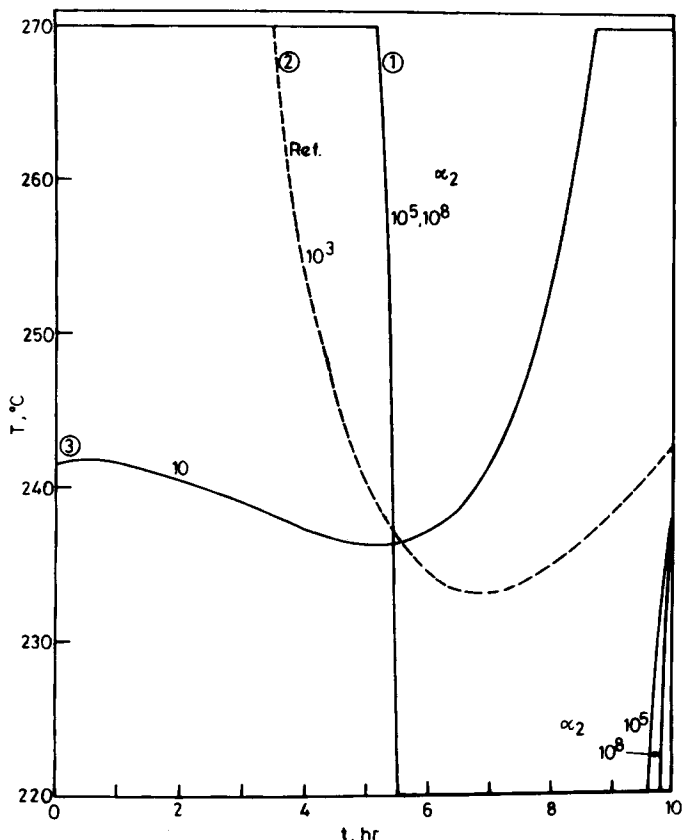


Fig. 4. Effect of α_2 on the optimal temperature profiles. Other parameters as in eq. (8). Values of final conversion (%), \overline{DP}_f and $[C_2(t_f)]$ are: (1) 78.7, 149.5, 0.0114; (2) reference, 76.7, 144.6, 0.0101; (3) 66.1, 111.6, 0.0078.

for a specified \overline{DP} and cyclic oligomer concentration. Mochizuki and Ito⁶ in their studies have clearly pointed out that the optimum profiles are extremely sensitive to the cyclization terms in the balance equations. For the objective function given in Eq. (1) in the initial portion of the reactor, the value of \overline{DP} is the lowest and the optimization algorithm tries to increase its value as rapidly as possible so as to minimize the contribution of $\overline{DP} - \overline{DP}_d$ in the objective function. After this initial region, the temperature drops in order to keep $[C_2(t_f)]$ low. The final increase in the optimal temperature profile occurs because of the $[C_1(t_f)]$ term in the objective function.

Figure 3 shows the effect of varying α_1 , the weighting factor for the cyclic dimer. It is observed that as α_1 increases, i.e., as we emphasize the importance of reducing the cyclic dimer concentration, the valley in the optimal temperature profiles increases in breadth and the final value of the cyclic dimer concentration decreases from 0.0135 to 0.00213 mol/kg. In fact, in the last two cases, the temperatures become so low that it is difficult to get a product of \overline{DP} equal to the desired value of 140, and an engineer must decide whether he can tolerate

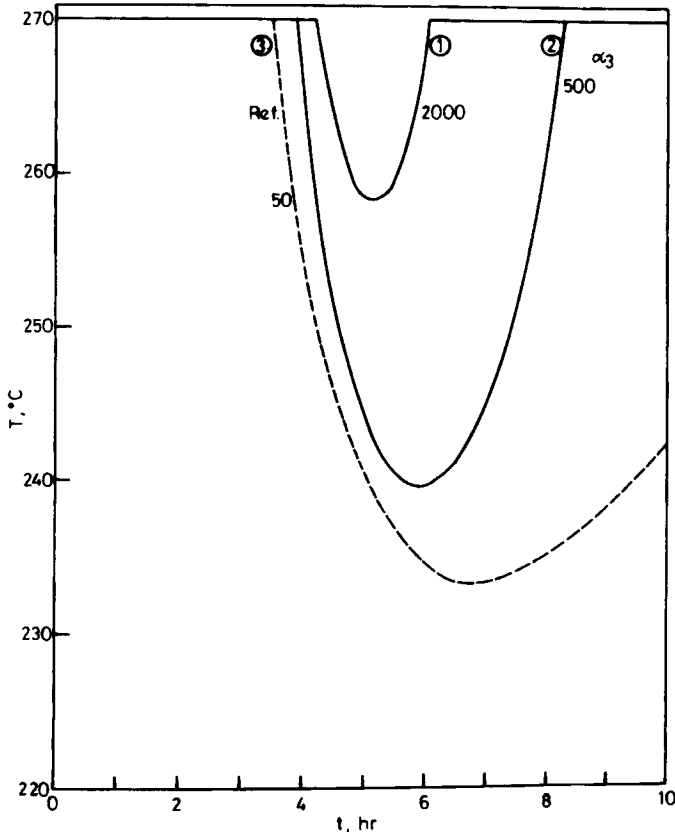


Fig. 5. Effect of α_3 on optimal temperature profiles. Other parameters as in eq. (8). Final conversion, \overline{DP}_f , and $[C_2(t_f)]$ are: (1) 88, 162.3, 0.018; (2) 84.5, 155.3, 0.0144; (3) Reference, 76.7, 144.6, 0.0101.

this variation. The behavior observed is consistent with our intuitive expectation that lower temperatures favor lower cyclic dimer concentrations.

Figure 4 shows the effect of the parameter α_2 , which represents the weight factor for \overline{DP} . A decrease in α_2 leads to lower initial temperatures. This is because by reducing α_2 the relative weight of the cyclic dimer production has increased and the effect is similar to that for curve 4 in Figure 3. It is interesting to observe that increasing α_2 does not drive the final value of \overline{DP} towards the value of 140, and this represents a complex interplay of the three contributions of the objective function corresponding to $[C_1]$, $[C_2]$, and \overline{DP} .

Figure 5 shows the effect of the weight α_3 of the monomer conversion on the optimal temperature profile. Since higher monomer conversions require higher temperatures, it is expected that an increase in α_3 leads to a more shallow valley in the temperature profile. Once again, however, this is accompanied by a larger deviation of \overline{DP}_f from the desired value of \overline{DP}_d , and an engineer must use his judgment on whether this value is tolerable. It is to be noted that as α_3 increases, the temperature near the exit of the reactor rises. This confirms our earlier contention that the final increase in the temperature is because of the conversion.

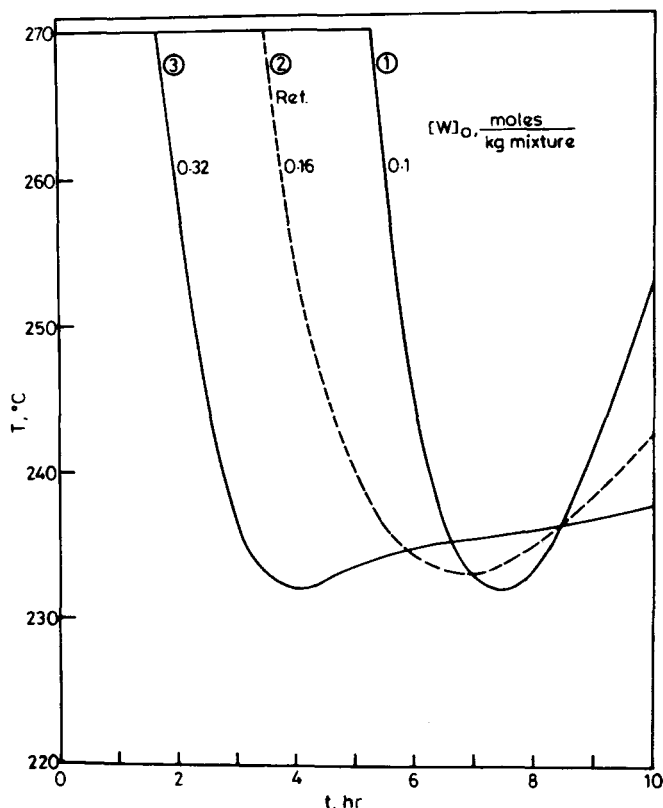


Fig. 6. Effect of feed water concentration on the optimal temperature profiles. Other parameters as in eq. (8). Conversion (%), \overline{DP}_f , and $[C_2(t_f)]$ are: (1) 63.6, 151.2, 0.0079; (2) Reference, 76.7, 144.6, 0.0101; (3) 88, 122, 0.0135.

In Figure 2 is shown the effect of varying the feed water concentration. Lower optimal temperatures are observed with higher feed-water concentrations. In earlier simulations of isothermal polymerization^{4,13,14} the following results were obtained: a higher feed water concentration gives a more rapid rise of \overline{DP} to a lower final value and a very rapid increase in conversion while a lower temperature gives a slower increase of both \overline{DP} and conversion with time to higher final values. The optimal temperature profiles shown in Figure 6 thus represent the result of the complex interplay of the three terms in the objective function.

Figure 7 shows the effect of varying the desired degree of polymerization, \overline{DP}_d , on the optimal temperature profile. Lower values of \overline{DP}_d lead to relatively lower temperatures. This is consistent with the observation on isothermal polymerizations⁴ that lower temperatures lead to a slower increase in \overline{DP} with time before equilibrium is attained. The deviation of the actual final value of \overline{DP}_f from the desired value \overline{DP}_d is to be noted.

Figure 8 shows how the optimum temperature profile changes as the total residence time t_f is varied. With larger residence times, lower temperatures are required to give the same final value of \overline{DP} . It is interesting to observe that the final values of the monomer conversion and the cyclic dimer concentration are

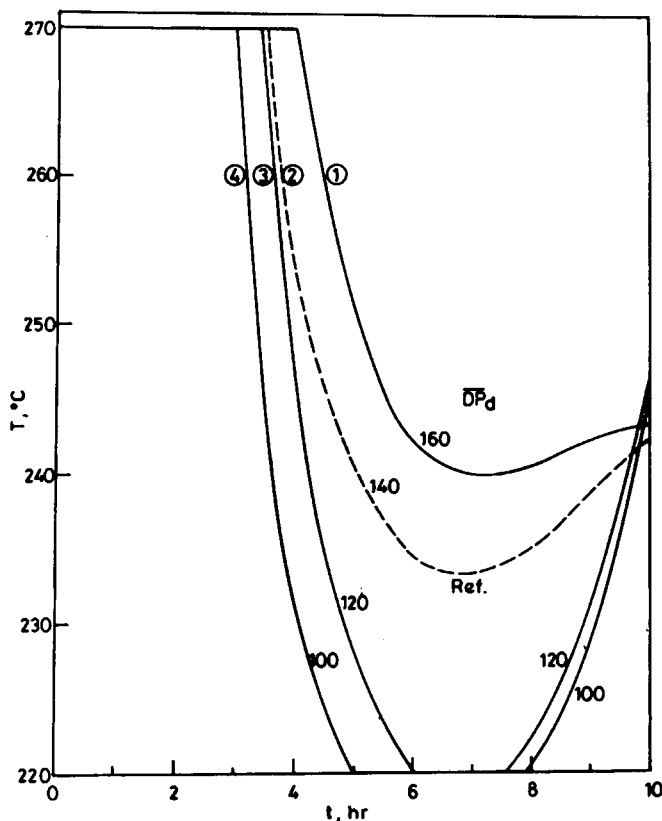


Fig. 7. Effect of \overline{DP}_d on the optimal temperature profiles. Other parameters as in eq. (8). Conversion (%), \overline{DP}_f and $[C_2(t_f)]$ are: (1) 80.6, 155.8, 0.0118; (2) Reference, 76.7, 144.6, 0.0101; (3) 71.7, 129.8, 0.0087; (4) 67, 117.3, 0.0074.

almost the same for all the runs. The objective function, however, is the lowest when $t_f = 8$ h.

Figure 9 shows the influence of adding some monofunctional acid stabilizers in the feed stream. Under isothermal conditions,¹⁵ the addition of these stabilizers decreases the \overline{DP} substantially and simultaneously speeds up the reaction. As expected from earlier studies,^{12,15} it is found that it is not possible to attain values of \overline{DP}_f of 140 in the presence of 1% concentration of A_1 and the optimal temperature profile is determined by the numerical values of $[C_1]$, $[C_2]$, and $[W]$. A higher temperature than shown in Figure 9 may lead to slightly higher values of \overline{DP}_f , but will be suboptimal due to the values of $[C_1(t_f)]$ and $[C_2]$. Once again it is found that optimality cannot easily be predicted using intuitive concepts developed on the basis of isothermal simulations.

A close study of Figures 6, 8, and 9 suggests the use of $[W]_0$, t_f , and $[A_1]_0$ to attain some type of a global optimum temperature profile, with $[W]_0$, $[A_1]_0$, and t_f used to attain the desired value of \overline{DP}_f . Some exploratory runs were taken keeping this in view, and it was found that for the following conditions,

$$t_f = 10 \text{ h}, \quad [A_1]_0 = 0.02 \text{ mol/kg}, \quad [W]_0 = 0.13 \text{ mol/kg} \quad (9)$$

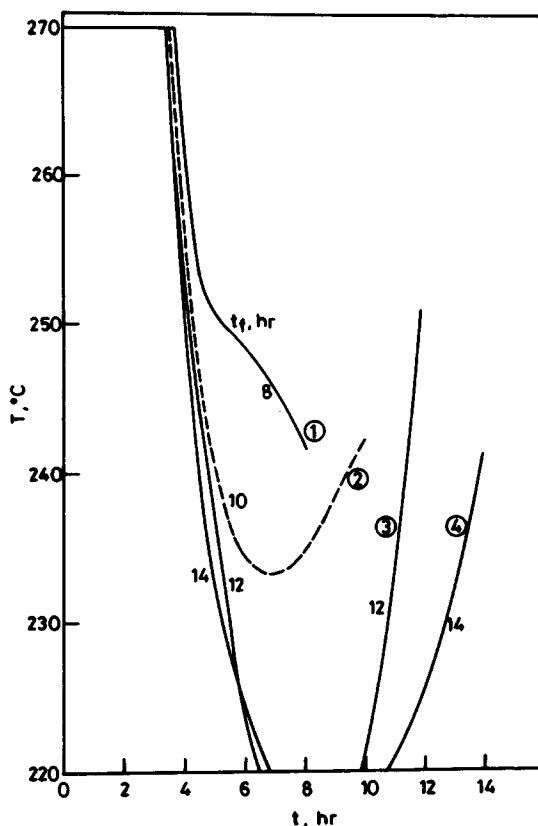


Fig. 8. Effect of varying the total residence time t_f on the optimal temperature profiles. Other parameters as in eq. (8). Values of conversion (%), \overline{DP}_f , and $[C_2(t_f)]$ are: (1) 76.9, 143.1, 0.0106; (2) Reference, 76.7, 144.6, 0.0101; (3) 76.2, 143.5, 0.0098; (4) 77, 147.5, 0.0098.

the optimal temperature profile gave $\overline{DP}_f = 134.2$, $[C_2(t_f)] = 0.0114$, and conversion = 80.6%, with the objective function being relatively low (2844) compared to other values.

CONCLUSIONS

A systematic study has been made to determine optimal temperature profiles for nylon 6 polymerization. An objective function different from those used earlier has been proposed which appears more reasonable and allows greater flexibility to an engineer. The parameters have been varied around a reference set of values, and it is found that a global optimal temperature profile may be obtained by choosing $[W]_0$, t_f , and $[A_1]_0$ appropriately. The optimal temperature profiles obtained are qualitatively different from those obtained by earlier workers, partly because of the cyclic dimerization step is different and partly because of the different objective function.

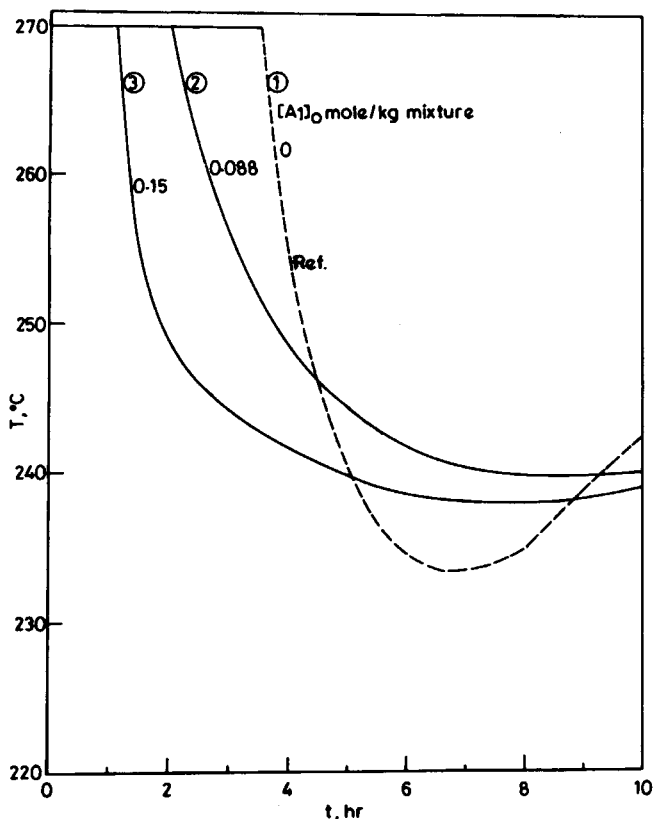


Fig. 9. Effect of varying monofunctional acid concentration in the feed. Other parameters as in eq. (8). Conversion (%), \overline{DP}_f , and $[C_2(t_f)]$ are: (1) Reference, 76.7, 144.6, 0.0101; (2) 86.5, 69.8, 0.0127; (3) 85.1, 45.45, 0.0108).

References

1. H. K. Reimschuessel, *J. Polym. Sci., Macromol. Rev.*, **12**, 65 (1977).
2. S. K. Gupta and A. Kumar, *Chem. Eng. Commun.*, (1983), to appear.
3. P. J. Hoftyzer, J. Hoogschagen, and D. W. van Krevelen, *Proc. 3rd Eur. Symp. Chem. Rxn. Eng.*, Amsterdam, 15-17 Sept., 1964, p. 247.
4. H. K. Reimschuessel and K. Nagasubramanian, *Chem. Eng. Sci.*, **27**, 1119 (1972).
5. W. F. H. Naudin ten Cate, *Proc. Int. Cong. Use of Elec. Computers in Chem. Eng.*, Paris, April, 1973.
6. S. Mochizuki and N. Ito, *Chem. Eng. Sci.*, **33**, 1401 (1978).
7. K. Tai, H. Teranishi, Y. Arai, and T. Tagawa, *J. Appl. Polym. Sci.*, **24**, 211 (1979).
8. K. Tai, H. Teranishi, Y. Arai, and T. Tagawa, *J. Appl. Polym. Sci.*, **25**, 77 (1980).
9. Y. Arai, K. Tai, H. Teranishi, and T. Tagawa, *Polymer*, **22**, 273 (1981).
10. K. Tai, Y. Arai, H. Teranishi, and T. Tagawa, *J. Appl. Polym. Sci.*, **25**, 1789 (1980).
11. K. Tai, Y. Arai and T. Tagawa, *J. Appl. Polym. Sci.*, **27**, 731 (1982).
12. M. V. Tirrell, G. H. Pearson, R. A. Weiss, and R. L. Laurence, *Polym. Eng. Sci.*, **15**, 386 (1975).
13. S. K. Gupta, A. Kumar, P. Tandon, and C. D. Naik, *Polymer*, **22**, 481 (1981).
14. S. K. Gupta, C. D. Naik, P. Tandon, and A. Kumar, *J. Appl. Polym. Sci.*, **26**, 2153 (1981).
15. S. K. Gupta, A. Kumar, and K. K. Agarwal, *J. Appl. Polym. Sci.*, **27**, 3089 (1982).
16. A. Ramagopal, A. Kumar, and S. K. Gupta, *Polym. Eng. Sci.*, **22**, 849 (1982).

17. S. K. Gupta, D. Kunzru, A. Kumar, and K. K. Agarwal, *J. Appl. Polym. Sci.*, **28**, 1625 (1983).
18. S. Mochizuki and N. Ito, *Chem. Eng. Sci.*, **28**, 1139 (1973).
19. J. M. Andrews, F. R. Jones, and J. A. Semlyen, *Polymer*, **15**, 420 (1974).
20. W. H. Ray and J. Szekeley, *Process Optimization*, 1st ed., Wiley, New York, 1973.
21. M. M. Denn, *Optimization by Variational Methods*, 1st ed., McGraw-Hill, New York, 1969.
22. J. Hicks, A. Mohan, and W. H. Ray, *Can. J. Chem. Eng.*, **47**, 590 (1969).
23. A. Kumar, V. K. Sukhthankar, C. P. Vaz, and S. K. Gupta, *Polym. Eng. Sci.*, **23**, (1983), to appear.
24. K. Tai and T. Tagawa, *J. Appl. Polym. Sci.*, **27**, 2791 (1982).

Received August 2, 1982

Accepted January 14, 1983